

There has been considerable work on tin halide-transition metal complexes but until recently very little on antimony halide-transition metal complexes. Recent crystal structures<sup>22</sup> have shown that various antimony halide-transition metal complexes have structures analogous to the tin halide complexes. For example, three Fe(*h*<sup>5</sup>-C<sub>5</sub>H<sub>5</sub>)(CO)<sub>2</sub> moieties will displace<sup>23</sup> chlorides on antimony chloride to give {[Fe(*h*<sup>5</sup>-C<sub>5</sub>H<sub>5</sub>)(CO)<sub>2</sub>]<sub>3</sub>SbCl<sub>5</sub>}<sup>+</sup>. We have found that ruthenocene reacts with SbCl<sub>5</sub> in the absence of oxygen to give a red-brown solid. This solid is fairly air sensitive, decomposing to a greenish yellow solid after a few minutes' exposure to air. As indicated above, it is our experience that the dark coloration (red-brown) of the reaction product is good testimony to the fact that the ruthenocene has been oxidized. The analytical data (see Table I) and ir spectrum of this red-brown compound (see Figure 3) indicate that the best formulation for this compound is [(cp)<sub>2</sub>RuCl](SbCl<sub>6</sub>). The similarity with the ir spectrum of [(cp)<sub>2</sub>RuI](I<sub>3</sub>) is striking, the exception being the Sb-Cl bands seen in the ~290-cm<sup>-1</sup> region. In addition, the instability of the complex is not surprising in light of the known<sup>18</sup> relative stabilities of the [Ru(cp)X]<sup>+</sup> cation (*i.e.*, I > Br > Cl).

The complex Fe(cpPPh<sub>2</sub>)<sub>2</sub> also reacts with SnX<sub>4</sub> (X = Cl, Br) to give compounds with compositions analogous (*i.e.*, 1:1 and 1:2 "adducts") to those found for ruthenocene (see Table I). The composition of the product formed with SbCl<sub>5</sub> is different. Molecular weight and electrochemical

(22) F. W. B. Einstein and R. D. G. Jones, *Inorg. Chem.*, **12**, 1690 (1973).

(23) Trinh-Troan and L. F. Dahl, *J. Amer. Chem. Soc.*, **93**, 2654 (1971).

measurements on these compounds show that dissolution of either Fe(cpPPh<sub>2</sub>)<sub>2</sub>·*n*SnX<sub>4</sub> (*n* = 1.5 or 2) or Fe(cpPPh<sub>2</sub>)<sub>2</sub>·*n*SbCl<sub>5</sub> (*n* = 1.5 or 3) leads to dissociation.

Infrared data for the Fe(cpPPh<sub>2</sub>)<sub>2</sub>·*n*SnX<sub>4</sub> compounds, as argued above for the HgX<sub>2</sub> compounds of this ferrocene, point to the presence of a P-Sn interaction. In contrast to the compound that we formulated as [(Ru(cp)<sub>2</sub>)<sub>2</sub>SnCl<sub>2</sub>](SnCl<sub>5</sub>)<sub>2</sub>, the ir spectrum of Fe(cpPPh<sub>2</sub>)<sub>2</sub>·1.5SnCl<sub>4</sub> only shows one broad Sn-Cl band with shoulders. The most probable formulation for Fe(cpPPh<sub>2</sub>)<sub>2</sub>·1.5SnX<sub>4</sub> is [(Fe(cpPPh<sub>2</sub>)<sub>2</sub>)<sub>2</sub>SnX<sub>2</sub>](SnX<sub>2</sub>)<sub>2</sub>. The SnX<sub>2</sub> bridging moiety in this system is bonded to the phosphorus atoms. Tin Mossbauer data are needed to check this formulation. Infrared data were inconclusive as to the molecular structures of the Fe(cpPPh<sub>2</sub>)<sub>2</sub>·1.5SbCl<sub>5</sub> stoichiometric compound and the compound formed with excess SbCl<sub>5</sub>, Fe(cpPPh<sub>2</sub>)<sub>2</sub>·3SbCl<sub>5</sub>.

Registry No. Fe(cpPPh<sub>2</sub>)<sub>2</sub>, 12150-46-8; Fe(cpPPh<sub>2</sub>)<sub>2</sub>·HgCl<sub>2</sub>, 50803-62-8; Fe(cpPPh<sub>2</sub>)<sub>2</sub>·2HgCl<sub>2</sub>, 50803-63-9; Fe(cpPPh<sub>2</sub>)<sub>2</sub>·HgBr<sub>2</sub>, 50803-59-3; Fe(cpPPh<sub>2</sub>)<sub>2</sub>·2HgBr<sub>2</sub>, 50803-60-6; Fe(cpPPh<sub>2</sub>)<sub>2</sub>·HgI<sub>2</sub>, 50803-65-1; Fe(cpPPh<sub>2</sub>)<sub>2</sub>·2HgI<sub>2</sub>, 50803-66-2; Fe(cpPPh<sub>2</sub>)<sub>2</sub>·Hg(SCN)<sub>2</sub>, 50803-69-5; [(Fe(cpPPh<sub>2</sub>)<sub>2</sub>)<sub>2</sub>Hg](BF<sub>4</sub>)<sub>2</sub>, 50803-76-4; [(Fe(cpPPh<sub>2</sub>)<sub>2</sub>)<sub>2</sub>Hg](PF<sub>6</sub>)<sub>2</sub>, 50803-77-5; [(Ru(cp)<sub>2</sub>)<sub>2</sub>SnCl<sub>2</sub>](SnCl<sub>5</sub>)<sub>2</sub>, 50803-54-8; [(Ru(cp)<sub>2</sub>)<sub>2</sub>SnBr<sub>2</sub>](SnBr<sub>5</sub>)<sub>2</sub>, 50803-53-7; [(Ru(cp)<sub>2</sub>Cl](SbCl<sub>6</sub>), 50803-39-9; Fe(cpCH<sub>3</sub>)<sub>2</sub>·6HgCl<sub>2</sub>, 50803-42-4; [Fe(cp-*n*-Bu)<sub>2</sub>·6HgCl<sub>2</sub>, 50803-52-6; Fe(cpPh)(cp)·7HgCl<sub>2</sub>, 50803-50-4; [(Fe(cpPPh<sub>2</sub>)<sub>2</sub>)<sub>2</sub>SnCl<sub>2</sub>](SnCl<sub>5</sub>)<sub>2</sub>, 50803-75-3; Fe(cpPPh<sub>2</sub>)<sub>2</sub>·2SnCl<sub>2</sub>, 50803-64-0; [(Fe(cpPPh<sub>2</sub>)<sub>2</sub>)<sub>2</sub>SnBr<sub>2</sub>](SnBr<sub>5</sub>)<sub>2</sub>, 50803-74-2; Fe(cpPPh<sub>2</sub>)<sub>2</sub>·2SnBr<sub>4</sub>, 50803-61-7; Fe(cpPPh<sub>2</sub>)<sub>2</sub>·1.5SbCl<sub>5</sub>, 50803-67-3; Fe(cpPPh<sub>2</sub>)<sub>2</sub>·3SbCl<sub>5</sub>, 50803-68-4; HgCl<sub>2</sub>, 7487-94-7; HgBr<sub>2</sub>, 7789-47-1; HgI<sub>2</sub>, 7774-29-0; Hg(SCN)<sub>2</sub>, 592-85-8; SnCl<sub>4</sub>, 7646-78-8; SnBr<sub>4</sub>, 7789-67-5; SbCl<sub>5</sub>, 7647-18-9; ruthenocene, 1287-13-4; Fe(cpCH<sub>3</sub>)<sub>2</sub>, 1291-47-0; Fe(cp-*n*-Bu)<sub>2</sub>, 1274-08-4; Fe(cpPh)(cp), 1287-25-8.

Contribution No. 4745 from the Arthur Amos Noyes Laboratory of Chemical Physics, California Institute of Technology, Pasadena, California 91109

## Crystal and Molecular Structure and 5°K Electronic Spectrum of Bis(tetraphenyldithioimidodiphosphinato)manganese(II)

OLAVI SIIMAN and HARRY B. GRAY\*

Received August 15, 1973

AIC306098

The crystal and molecular structure of bis(tetraphenyldithioimidodiphosphinato)manganese(II) has been determined by single-crystal X-ray diffraction methods. The pink crystals, which form as rectangular prisms, belong to space group P1 with *a* = 13.550 (4) Å, *b* = 14.334 (4) Å, *c* = 13.824 (3) Å, α = 82.17 (2)°, β = 110.50 (2)°, γ = 114.11 (2)°, and Z = 2 for the Dirichlet reduced cell. Full-matrix least-squares refinement on 8526 nonzero reflections produced a converged solution with R<sub>F</sub> = 5.8%. The complex is monomeric and consists of four sulfur atoms in an approximately tetrahedral arrangement about the manganese atom. The two MnS<sub>2</sub>P<sub>2</sub>N chelate rings have twisted boat conformations with sulfur and phosphorus atoms at the apices. The single-crystal electronic absorption spectra at 77 and 5°K of the tetrahedral Mn<sup>II</sup>S<sub>4</sub> complex have been measured between 13,000 and 30,000 cm<sup>-1</sup>. Transitions from the <sup>6</sup>A<sub>1</sub> ground state to quartet excited states derived from the <sup>4</sup>G, <sup>4</sup>D, and <sup>4</sup>P Mn<sup>2+</sup> levels are observed. The experimental transition energies are in excellent agreement with those calculated assuming 10Dq = -4685.6, B = 559.2, and C = 3118.7 cm<sup>-1</sup>. Vibrational progressions in quanta of the a<sub>1</sub> Mn-S stretch (average spacing 254 cm<sup>-1</sup>; ground state 242 cm<sup>-1</sup>) are built on four electronic origins in the <sup>6</sup>A<sub>1</sub> → <sup>4</sup>E, <sup>4</sup>A<sub>1</sub> (<sup>4</sup>G) system. The lowest three origins (21,139; 21,186.5; 21,272.5 cm<sup>-1</sup>) are assigned to transitions to the spin-orbit components of <sup>4</sup>E(<sup>4</sup>G), whereas the origin at 21,346 cm<sup>-1</sup> is attributed to <sup>6</sup>A<sub>1</sub> → <sup>4</sup>A<sub>1</sub>(<sup>4</sup>G).

Four-coordinate complexes of the type M(SPPPh<sub>2</sub>NPPPh<sub>2</sub>S)<sub>2</sub>, where R = Me or Ph and M = Fe(II), Co(II), Ni(II), or Zn(II), have been reported<sup>1</sup> recently. Crystal structure studies have established tetrahedral MS<sub>4</sub> coordination for both the Ni(II)<sup>2</sup> and Fe(II)<sup>3</sup> chelates with R = Me. We have

extended the synthetic and structural investigation of this series to include Mn(SPPPh<sub>2</sub>NPPPh<sub>2</sub>S)<sub>2</sub>. In addition to a single-crystal X-ray structure analysis, we have measured and interpreted the 5°K single-crystal electronic absorption spectrum of this tetrahedral Mn<sup>II</sup>S<sub>4</sub> complex. A preliminary

(1) A. Davison and E. S. Switkes, *Inorg. Chem.*, **10**, 837 (1971).

(2) M. R. Churchill, J. Cooke, J. P. Fennessey, and J. Wormald, *Inorg. Chem.*, **10**, 1031 (1971).

(3) M. R. Churchill and J. Wormald, *Inorg. Chem.*, **10**, 1778 (1971).

account of the X-ray structural part of this work has appeared.<sup>4</sup>

### Experimental Section

Bis(tetraphenyldithioimidodiphosphinato)manganese(II) was prepared as described previously.<sup>4</sup> *Anal.* Calcd for  $C_{48}H_{40}N_2MnP_4S_4$ : C, 60.56; H, 4.24; N, 2.94; Mn, 5.77; P, 13.02; S, 13.47. Found: C, 60.20; H, 4.14; N, 2.87; Mn, 5.74; P, 12.93; S, 13.99.

Slow evaporation of a 1:10 hexane-dichloromethane solution of bis(tetraphenyldithioimidodiphosphinato)manganese(II) produced single crystals suitable for X-ray study. Pink crystals in the form of rectangular prisms were mounted along the *a*, *b*, and *c* axes for Weissenberg photography with  $Cu K\alpha$  radiation. Photographs of the  $h(0-2)l$ ,  $hk(0-2)$ , and  $(0-2)kl$  zones revealed no systematic absences other than those showing that the normals to the crystal faces defined a body-centered cell (extinctions for  $h+k+l=2n+1$ ) in the triclinic space group  $I1$  or  $I\bar{1}$ . The unit cell data (primitive cell hereafter) are given in Table I.

Data were collected for a crystal of approximate dimensions  $0.5 \times 0.1 \times 0.1$  mm on a Daxex-automated Syntex full-circle diffractometer equipped with a graphite crystal incident-beam monochromator for  $Mo K\alpha$  radiation. The crystal was mounted with its *a* axis parallel to the  $\phi$  axis of the diffractometer. Intensity measurements were made by the  $\theta-2\theta$  scan technique at a scan rate which varied linearly from  $1/2$  to  $4^\circ/\text{min}$  between 5 and 2000 counts/sec determined at the peak maximum. Below 5 counts/sec the scan rate was  $1/2^\circ/\text{min}$  and above 2000 counts/sec it was  $4^\circ/\text{min}$ . The scan width varied linearly from 1.7 to  $2.0^\circ$  over the  $2\theta$  range, 10.0–40.0°. Background counts of half the peak scan time were taken at the extremes of each scan. Three check reflections were monitored after every 24 reflections. An average reduction of about 2.5% was noted for these reflections over the intensity record.

A total of 8526 independent reflections in the range  $0.035 < \sin \theta < 0.43$  for  $Mo K\alpha$  radiation were recorded in 14 sets in reciprocal space for one crystal. The reflections in each set were scaled to an arbitrary  $|F|$  (chosen as the average value of one of the check reflections) for all data sets. Standard deviations in the intensities were estimated according to the formula

$$\sigma(I_0) = [S + B_1 + B_2 + (0.01(S - B_1 - B_2))^2]^{1/2}$$

where *S* is the peak count and *B*<sub>1</sub> and *B*<sub>2</sub> are the background counts on either side of the peak. The values *I*<sub>0</sub> and  $\sigma(I_0)$  were corrected for Lorentz and polarization effects. No absorption correction was made ( $\mu_{\text{max}} \sim 0.2$ ) since the linear absorption coefficient for  $Mo K\alpha$  radiation was  $6.5 \text{ cm}^{-1}$ . The  $|F|$  values were put on an approximately absolute scale by use of a Wilson plot<sup>5</sup> from which a scale factor and an overall thermal parameter ( $B = 3.52 \text{ \AA}^2$ ) were obtained. The zero moment test<sup>6</sup> and the test<sup>7</sup> for distribution of  $|E|$  values indicated a centric structure (*i.e.*, triclinic space group  $I\bar{1}$ ) as confirmed by later solution and refinement.

Single crystals of  $Mn(SPPH_2NPPH_2S)_2$  used for the spectroscopic studies were  $\sim 0.50$ – $0.75$  mm thick and had a cross section of  $\sim 1 \times 4 \text{ mm}^2$ . Electronic spectra between 13,000 and  $30,000 \text{ cm}^{-1}$  were recorded with a Cary 17 spectrophotometer. Single-crystal electronic spectra at  $5^\circ \text{K}$  were obtained using an Andonian Associates liquid helium dewar placed in the sample beam following a double-Glan air-spaced calcite polarizing prism. The electronic absorption bands were observed not to be polarized significantly along the extinction directions of the crystals.

### Solution and Refinement of the Structure

The positions of the manganese, sulfur, and phosphorus atoms were determined from a three-dimensional Patterson map, sharpened to remove the  $\theta$  dependence in  $|F_0|$  and with the origin peak subtracted. When the positional and estimated isotropic thermal parameters of the Mn, S, and P atoms were introduced into a structure factor calculation, an *R* index

$$\Sigma ||F_0| - |F_c|| / \Sigma |F_0| = 0.383$$

resulted. A three-dimensional difference Fourier synthesis revealed the positions of all nitrogen and carbon atoms. When these atoms

(4) O. Siiman, M. Wrighton, and H. B. Gray, *J. Coord. Chem.*, **2**, 159 (1972).

(5) A. J. C. Wilson, *Nature (London)*, **150**, 152 (1942).

(6) E. R. Howells, D. C. Phillips, and D. Rogers, *Acta Crystallogr.*, **3**, 210 (1950).

(7) H. Hauptman, J. Fischer, H. Hancock, and D. A. Norton, *Acta Crystallogr., Sect. B*, **25**, 811 (1969).

Table I. Unit Cell Data for  $Mn(SPPH_2NPPH_2S)_2$ <sup>a</sup>

<i>a</i> = 13.550 (4) Å	$\alpha$ = 82.17 (2)°
<i>b</i> = 14.334 (4) Å	$\beta$ = 110.50 (2)
<i>c</i> = 13.824 (3) Å	$\gamma$ = 114.11 (2)
Triclinic	<i>Z</i> = 2
Space group $P1$ or $P\bar{1}$	<i>V</i> = 2295.3 (1.8) Å <sup>3</sup>
Mol wt 951.97	$\rho_o$ = 1.37 (2) g cm <sup>-3</sup> <sup>b</sup>
	$\rho_c$ = 1.377 g cm <sup>-3</sup>

<sup>a</sup> The cell dimensions were obtained from a least-squares refinement of  $2\theta$  values of 23 high-angle reflections ( $2\theta > 26.6^\circ$ ,  $Mo K\alpha$ ) centered on the diffractometer. <sup>b</sup> Measured by flotation in aqueous potassium iodide solutions at  $23^\circ$ .

were introduced, the *R* index decreased to 0.224. All crystallographic calculations were performed on an IBM 370-155 computer using subprograms operating under the CRYM system.<sup>8</sup>

Least-squares refinement minimized the quantity  $\Sigma w(F_o^2 - F_c^2)^2$  where the weight, *w*, is  $1/\sigma^2(F_o^2)$ . Nonhydrogen and hydrogen atomic scattering factors were those calculated by Cromer and Waber<sup>9</sup> and Stewart, *et. al.*,<sup>10</sup> respectively. Correction for the real part of the anomalous dispersion effects for Mn, S, and P was included in the calculation with values of  $\Delta f'$  from Cromer's compilation.<sup>11</sup>

Four cycles of full-matrix least-squares refinement reduced the *R* index to 0.119, whereupon three cycles, in which anisotropic thermal parameters were assigned to all nonhydrogen atoms, yielded an *R* value of 0.073. Difference Fourier maps evaluated in the planes of the six carbon atoms of each phenyl group revealed the positions of the five hydrogen atoms of each phenyl ring. For the purposes of further least-squares refinement, however, the hydrogen atoms were positioned so that each was in the plane of the three nearest carbon atoms, 1.09 Å away from the apical carbon atom and equidistant from the other two carbons. The assigned positional and isotropic thermal parameters ( $B = 5.0 \text{ \AA}^2$ ) of the hydrogen atoms were not refined but were updated after each least-squares cycle. Two cycles of least-squares refinement with inclusion of the hydrogen atoms lowered the *R* index to 0.064. At this point classes of reflections based on  $|F_o|$ , Miller indices, and  $(\sin \theta)/\lambda$  were analyzed for trends in average values of  $\Sigma w(F_o^2 - F_c^2)^2$ . No systematic trends were observed; however, 16 random reflections had comparatively high weighted residuals ( $>15$ ) or  $F^2 < -100$  and were given zero weight in the final refinements. Inspection of some low-angle intense reflections indicated that inclusion of a secondary extinction coefficient was justified. Another two cycles of refinement, including a secondary extinction factor, yielded convergence at an *R* index of 0.058 and a goodness-of-fit of 2.0. The final value of the secondary extinction coefficient,<sup>12</sup> *g*, was  $5.5 \times 10^{-4}$ . A final difference Fourier map showed no peak higher than  $0.35 \text{ e \AA}^{-3}$  or atoms in the earlier difference map.

The final positional and thermal parameters of the heavy atoms are listed in Table II. The assumed hydrogen atom positions as included in the final structure factor calculation are given in Table III.

### Description of the Structure

A stereoscopic view of the molecule is presented in Figure 1. Interatomic distances and their estimated standard deviations are set out in Table IV. Bond angles are given in Table V. Planes defined by the manganese and sulfur atoms of each chelate ring are given in Table VI. The greatest deviation of a carbon atom from the least squares plane of a phenyl ring is 0.0118 Å. The root-mean-square amplitudes of vibration along the principal axes of thermal motion for the atoms that were refined anisotropically are given in Table VII.

The structure consists of monomeric units of  $Mn(SPPH_2NPPH_2S)_2$  in which the central metal is in approximately tetrahedral coordination to four sulfur atoms. The deviation

(8) D. J. Duchamp, Paper B-14, American Crystallographic Association Meeting, Bozeman, Mont., 1964, p 29.

(9) D. T. Cromer and J. T. Waber, *Acta Crystallogr.*, **18**, 104 (1965).

(10) R. F. Stewart, E. R. Davidson, and W. T. Simpson, *J. Chem. Phys.*, **42**, 3175 (1965).

(11) D. T. Cromer, *Acta Crystallogr.*, **18**, 17 (1965).

(12) A. C. Larson, *Acta Crystallogr.*, **23**, 664 (1967).

Table II. Positional and Thermal Parameters of the Nonhydrogen Atoms and Their Standard Deviations<sup>a</sup>

	<i>x</i>	<i>y</i>	<i>z</i>	$\beta_{11}$	$\beta_{22}$	$\beta_{33}$	$\beta_{12}$	$\beta_{13}$	$\beta_{23}$
Mn	-0.11428 (4)	0.24823 (3)	0.22447 (4)	0.00648 (4)	0.00647 (3)	0.00647 (4)	0.00562 (6)	0.00413 (7)	-0.00067 (5)
S(1)	-0.12450 (7)	0.40227 (6)	0.26929 (6)	0.00646 (7)	0.00558 (5)	0.00758 (6)	0.00394 (11)	0.00494 (11)	-0.00069 (9)
S(2)	-0.30001 (7)	0.10752 (6)	0.17854 (6)	0.00742 (8)	0.00508 (5)	0.00738 (6)	0.00538 (11)	0.00426 (12)	-0.00045 (9)
S(3)	-0.04521 (7)	0.27886 (6)	0.07613 (6)	0.00557 (7)	0.00817 (6)	0.00533 (6)	0.00327 (11)	0.00197 (11)	-0.00107 (9)
S(4)	0.01344 (8)	0.20140 (7)	0.37930 (6)	0.00952 (9)	0.00910 (7)	0.00554 (6)	0.01075 (13)	0.00502 (12)	-0.00070 (10)
P(1)	-0.26418 (7)	0.33436 (5)	0.31414 (6)	0.00641 (7)	0.00459 (5)	0.00479 (5)	0.00424 (10)	0.00274 (10)	-0.00126 (8)
P(2)	-0.41213 (7)	0.17315 (5)	0.15801 (6)	0.00594 (7)	0.00423 (5)	0.00477 (5)	0.00284 (10)	0.00368 (10)	-0.00124 (8)
P(3)	0.12206 (7)	0.32436 (5)	0.15729 (6)	0.00559 (7)	0.00443 (5)	0.00467 (5)	0.00339 (10)	0.00269 (10)	0.00028 (8)
P(4)	0.10715 (7)	0.16773 (5)	0.31505 (6)	0.00633 (7)	0.00451 (5)	0.00444 (5)	0.00449 (10)	0.00342 (10)	0.00024 (8)
N(1)	-0.3794 (2)	0.2618 (2)	0.2351 (2)	0.0066 (2)	0.0056 (2)	0.0058 (2)	0.0033 (3)	0.0038 (3)	-0.0033 (3)
N(2)	0.1640 (2)	0.2474 (2)	0.2390 (2)	0.0068 (2)	0.0052 (2)	0.0065 (2)	0.0046 (3)	0.0053 (3)	0.0026 (3)
C(1)	-0.2966 (3)	0.4346 (2)	0.3453 (2)	0.0071 (3)	0.0049 (2)	0.0042 (2)	0.0051 (4)	0.0024 (4)	-0.0004 (3)
C(2)	-0.2117 (3)	0.5228 (2)	0.3953 (2)	0.0089 (3)	0.0066 (2)	0.0085 (3)	0.0051 (5)	0.0018 (5)	-0.0058 (4)
C(3)	-0.2369 (3)	0.5983 (2)	0.4200 (3)	0.0134 (4)	0.0066 (2)	0.0088 (3)	0.0073 (6)	0.0024 (6)	-0.0061 (4)
C(4)	-0.3478 (4)	0.5870 (3)	0.3947 (3)	0.0160 (5)	0.0079 (3)	0.0086 (3)	0.0150 (7)	0.0039 (6)	-0.0027 (4)
C(5)	-0.4334 (3)	0.5005 (3)	0.3444 (3)	0.0109 (4)	0.0107 (3)	0.0141 (4)	0.0143 (6)	0.0005 (7)	-0.0067 (6)
C(6)	-0.4074 (3)	0.4246 (2)	0.3197 (3)	0.0078 (3)	0.0069 (2)	0.0100 (3)	0.0067 (5)	0.0003 (5)	-0.0059 (4)
C(7)	-0.2250 (3)	0.2685 (2)	0.4340 (2)	0.0091 (3)	0.0061 (2)	0.0058 (2)	0.0081 (5)	0.0044 (5)	-0.0002 (4)
C(8)	-0.3033 (3)	0.1780 (2)	0.4550 (2)	0.0138 (4)	0.0063 (2)	0.0070 (3)	0.0060 (5)	0.0076 (6)	0.0003 (4)
C(9)	-0.2709 (4)	0.1274 (3)	0.5481 (3)	0.0192 (6)	0.0069 (3)	0.0095 (3)	0.0080 (7)	0.0127 (7)	0.0024 (5)
C(10)	-0.1631 (4)	0.1683 (3)	0.6147 (3)	0.0185 (6)	0.0112 (4)	0.0080 (3)	0.0171 (8)	0.0098 (7)	0.0059 (5)
C(11)	-0.0855 (4)	0.2579 (3)	0.5953 (3)	0.0134 (5)	0.0154 (4)	0.0082 (3)	0.0128 (8)	0.0004 (7)	0.0047 (6)
C(12)	-0.1168 (3)	0.3084 (3)	0.5042 (3)	0.0107 (4)	0.0109 (3)	0.0070 (3)	0.0082 (6)	0.0023 (6)	0.0041 (5)
C(13)	-0.5443 (3)	0.0729 (2)	0.1640 (2)	0.0078 (3)	0.0047 (2)	0.0050 (2)	0.0027 (4)	0.0060 (4)	-0.0007 (3)
C(14)	-0.5792 (3)	-0.0241 (2)	0.1264 (3)	0.0092 (4)	0.0054 (2)	0.0103 (3)	0.0018 (5)	0.0089 (5)	-0.0046 (4)
C(15)	-0.6855 (3)	-0.0975 (2)	0.1229 (3)	0.0131 (5)	0.0051 (2)	0.0116 (3)	-0.0020 (5)	0.0133 (7)	-0.0039 (4)
C(16)	-0.7560 (3)	-0.0758 (3)	0.1563 (3)	0.0138 (5)	0.0081 (3)	0.0161 (4)	-0.0069 (6)	0.0229 (8)	-0.0073 (6)
C(17)	-0.7211 (4)	0.0189 (3)	0.1961 (4)	0.0159 (5)	0.0108 (4)	0.0227 (6)	-0.0031 (7)	0.0318 (10)	-0.0106 (7)
C(18)	-0.6154 (3)	0.0935 (2)	0.2001 (3)	0.0125 (4)	0.0057 (2)	0.0140 (4)	-0.0002 (5)	0.0182 (7)	-0.0053 (5)
C(19)	-0.4456 (2)	0.2211 (2)	0.0274 (2)	0.0063 (3)	0.0046 (2)	0.0050 (2)	0.0045 (4)	0.0031 (4)	-0.0009 (3)
C(20)	-0.5460 (3)	0.1697 (2)	-0.0501 (2)	0.0077 (3)	0.0066 (2)	0.0059 (2)	0.0040 (5)	0.0030 (5)	-0.0010 (4)
C(21)	-0.5643 (3)	0.2080 (3)	-0.1498 (2)	0.0099 (4)	0.0101 (3)	0.0054 (2)	0.0080 (6)	-0.0002 (5)	-0.0014 (4)
C(22)	-0.4855 (4)	0.2959 (3)	-0.1716 (2)	0.0141 (5)	0.0098 (3)	0.0061 (3)	0.0115 (7)	0.0055 (6)	0.0046 (4)
C(23)	-0.3873 (3)	0.3481 (3)	-0.0953 (3)	0.0126 (4)	0.0078 (3)	0.0083 (3)	0.0032 (6)	0.0061 (6)	0.0052 (4)
C(24)	-0.3669 (3)	0.3115 (2)	0.0045 (2)	0.0087 (3)	0.0064 (2)	0.0065 (2)	0.0015 (5)	0.0028 (5)	0.0014 (4)
C(25)	0.2023 (2)	0.3523 (2)	0.0693 (2)	0.0064 (3)	0.0041 (2)	0.0049 (2)	0.0033 (4)	0.0033 (4)	-0.0005 (3)
C(26)	0.1681 (3)	0.3928 (2)	-0.0278 (2)	0.0104 (4)	0.0076 (2)	0.0069 (3)	0.0101 (5)	0.0074 (5)	0.0035 (4)
C(27)	0.2368 (3)	0.4187 (2)	-0.0907 (2)	0.0158 (5)	0.0077 (3)	0.0073 (3)	0.0119 (6)	0.0130 (6)	0.0057 (4)
C(28)	0.3366 (3)	0.4044 (2)	-0.0576 (3)	0.0121 (4)	0.0060 (2)	0.0094 (3)	0.0046 (5)	0.0138 (6)	0.0008 (4)
C(29)	0.3707 (3)	0.3642 (3)	0.0374 (3)	0.0083 (3)	0.0096 (3)	0.0096 (3)	0.0079 (5)	0.0090 (6)	0.0014 (5)
C(30)	0.3032 (3)	0.3378 (2)	0.1005 (2)	0.0079 (3)	0.0082 (3)	0.0060 (2)	0.0075 (5)	0.0046 (5)	0.0020 (4)
C(31)	0.1684 (2)	0.4454 (2)	0.2200 (2)	0.0059 (3)	0.0050 (2)	0.0053 (2)	0.0043 (4)	0.0043 (4)	0.0000 (3)
C(32)	0.1237 (3)	0.5170 (2)	0.1722 (2)	0.0098 (4)	0.0066 (2)	0.0079 (3)	0.0078 (5)	0.0018 (5)	-0.0010 (4)
C(33)	0.1638 (3)	0.6110 (2)	0.2181 (3)	0.0134 (5)	0.0062 (3)	0.0127 (4)	0.0106 (6)	0.0056 (7)	-0.0001 (5)
C(34)	0.2471 (3)	0.6328 (3)	0.3127 (3)	0.0145 (5)	0.0064 (3)	0.0109 (3)	0.0066 (6)	0.0085 (7)	-0.0049 (5)
C(35)	0.2917 (3)	0.5631 (3)	0.3611 (2)	0.0137 (5)	0.0075 (3)	0.0065 (3)	0.0055 (6)	0.0017 (6)	-0.0037 (4)
C(36)	0.2521 (3)	0.4685 (2)	0.3154 (2)	0.0102 (4)	0.0061 (2)	0.0057 (2)	0.0058 (5)	0.0023 (5)	-0.0012 (4)
C(37)	0.2253 (3)	0.1525 (2)	0.4192 (2)	0.0075 (3)	0.0051 (2)	0.0045 (2)	0.0059 (4)	0.0026 (4)	-0.0006 (3)
C(38)	0.2084 (3)	0.0937 (3)	0.5049 (2)	0.0101 (4)	0.0097 (3)	0.0060 (2)	0.0077 (6)	0.0046 (5)	0.0030 (4)
C(39)	0.3003 (4)	0.0831 (3)	0.5844 (2)	0.0154 (5)	0.0124 (4)	0.0049 (2)	0.0146 (8)	0.0008 (6)	0.0035 (5)
C(40)	0.4083 (3)	0.1318 (3)	0.5800 (3)	0.0116 (4)	0.0117 (4)	0.0070 (3)	0.0137 (7)	-0.0035 (6)	-0.0027 (5)
C(41)	0.4259 (3)	0.1902 (3)	0.4966 (3)	0.0079 (4)	0.0111 (3)	0.0095 (3)	0.0090 (6)	0.0010 (6)	-0.0012 (5)
C(42)	0.3354 (3)	0.2003 (2)	0.4163 (2)	0.0075 (3)	0.0080 (3)	0.0065 (2)	0.0073 (5)	0.0032 (5)	0.0010 (4)
C(43)	0.0184 (2)	0.0449 (2)	0.2505 (2)	0.0064 (3)	0.0046 (2)	0.0059 (2)	0.0040 (4)	0.0045 (4)	-0.0001 (3)
C(44)	0.0045 (5)	0.0320 (3)	0.1525 (3)	0.0314 (8)	0.0067 (3)	0.0081 (3)	-0.0018 (8)	0.0167 (9)	-0.0037 (5)
C(45)	-0.0672 (6)	-0.0605 (3)	0.1031 (3)	0.0472 (13)	0.0092 (4)	0.0094 (4)	-0.0029 (11)	0.0170 (12)	-0.0082 (6)
C(46)	-0.1239 (4)	-0.1400 (3)	0.1494 (4)	0.0179 (6)	0.0070 (3)	0.0144 (4)	0.0015 (7)	0.0018 (9)	-0.0080 (6)
C(47)	-0.1119 (4)	-0.1297 (3)	0.2464 (4)	0.0111 (5)	0.0058 (3)	0.0171 (5)	-0.0022 (6)	0.0086 (8)	0.0012 (6)
C(48)	-0.0417 (3)	-0.0373 (3)	0.2977 (3)	0.0138 (5)	0.0080 (3)	0.0098 (3)	0.0001 (6)	0.0112 (7)	0.0005 (5)

<sup>a</sup> The standard deviations given in parentheses refer to the last digit of the respective values. The anisotropic thermal parameter is defined as  $\exp[-(\beta_{11}h^2 + \beta_{22}k^2 + \beta_{33}l^2 + \beta_{12}hk + \beta_{13}hl + \beta_{23}kl)]$ .

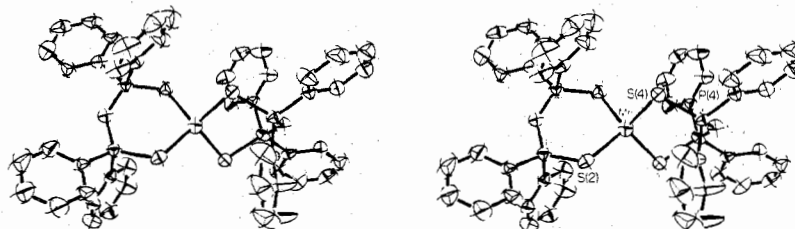


Figure 1. A stereoscopic view of the Mn(SPPPh<sub>2</sub>NPPPh<sub>2</sub>S)<sub>2</sub> molecule. Thermal ellipsoids are drawn at the 50% probability level.

of the S-Mn-S angles from 109.5° ranges from +2.6 to -3.2°. The angle between the S(1)-Mn-S(2) and S(3)-

Mn-S(4) planes is 86.8°. Interligand angles from S(2), S(2)-Mn-S(3) = 107.47° and S(2)-Mn-S(4) = 108.48°,

Table III. Positional Parameters Generated for Hydrogen Atoms<sup>a</sup>

Atom	x	y	z	
C(2)	H(1)	-0.1225	0.5330	0.4158
C(3)	H(2)	-0.1680	0.6674	0.4598
C(4)	H(3)	-0.3680	0.6466	0.4146
C(5)	H(4)	-0.5224	0.4910	0.3237
C(6)	H(5)	-0.4764	0.3559	0.2793
C(8)	H(6)	-0.3896	0.1455	0.4002
C(9)	H(7)	-0.3322	0.0557	0.5663
C(10)	H(8)	-0.1382	0.1280	0.6859
C(11)	H(9)	0.0005	0.2900	0.6506
C(12)	H(10)	-0.0548	0.3808	0.4880
C(14)	H(11)	-0.5227	-0.0426	0.0995
C(15)	H(12)	-0.7124	-0.1737	0.0929
C(16)	H(13)	-0.8405	-0.1335	0.1515
C(17)	H(14)	-0.7773	0.0357	0.2252
C(18)	H(15)	-0.5887	0.1689	0.2319
C(20)	H(16)	-0.6102	0.0995	-0.0331
C(21)	H(17)	-0.6428	0.1672	-0.2112
C(22)	H(18)	-0.5007	0.3249	-0.2503
C(23)	H(19)	-0.3247	0.4190	-0.1132
C(24)	H(20)	-0.2886	0.3539	0.0652
C(26)	H(21)	0.0881	0.4044	-0.0550
C(27)	H(22)	0.2101	0.4507	-0.1669
C(28)	H(23)	0.3895	0.4251	-0.1073
C(29)	H(24)	0.4508	0.3529	0.0638
C(30)	H(25)	0.3306	0.3050	0.1761
C(32)	H(26)	0.0562	0.4993	0.0975
C(33)	H(27)	0.1292	0.6677	0.1791
C(34)	H(28)	0.2779	0.7067	0.3493
C(35)	H(29)	0.3588	0.5814	0.4361
C(36)	H(30)	0.2873	0.4122	0.3550
C(38)	H(31)	0.1223	0.0554	0.5098
C(39)	H(32)	0.2857	0.0356	0.6507
C(40)	H(33)	0.4804	0.1241	0.6429
C(41)	H(34)	0.5125	0.2294	0.4931
C(42)	H(35)	0.3512	0.2466	0.3498
C(44)	H(36)	0.0503	0.0952	0.1109
C(45)	H(37)	-0.0773	-0.0681	0.0224
C(46)	H(38)	-0.1793	-0.2124	0.1084
C(47)	H(39)	-0.1577	-0.1945	0.2868
C(48)	H(40)	-0.0344	-0.0301	0.3776

<sup>a</sup> The phenyl group hydrogen atoms were assigned positions in the plane of the three nearest carbon atoms, 1.09 Å away from the apical carbon atom and equidistant from the other two carbons. The isotropic thermal parameter for the hydrogen atoms was given the value  $B = 5.0 \text{ \AA}^2$ .

are both less than the tetrahedral value, whereas angles from S(1), S(1)-Mn-S(3) = 110.82° and S(1)-Mn-S(4) = 106.32°, deviate above and below 109.5°. One short Mn-S(2) bond distance of 2.426 Å is compensated by an opening of the Mn-S(2)-P(2) = 104.56° angle so that the conformations of the two chelate rings are almost identical, as seen from the deviations of P, N, and C atoms from the two S-Mn-S planes. The two MnS<sub>2</sub>P<sub>2</sub>N chelate rings are arranged in twisted boat conformations with sulfur and phosphorus atoms at the apices. In this conformation the interactions between phenyl groups on different phosphorus atoms but in the same chelate ring are axial-equatorial. The chair conformations and boats with metal and nitrogen atoms at the ends have unfavorable axial phenyl-phenyl contacts and are more crowded sterically than the twisted boat that is observed. The molecule as a whole approximates S<sub>4</sub> point symmetry; *i.e.*, the positions of the phenyl groups, axial or equatorial, and puckering of the six-membered chelate rings satisfy the conditions for an improper fourfold axis of rotation along N(1)-Mn-N(2).

The average bond distances and bond angles and their root mean-squares deviations are Mn-S = 2.443 (12), S-P = 2.013 (5), P-N = 1.588 (6), and P-C = 1.815 (8) Å and S-Mn-S = 109.5 (2.2), Mn-S-P = 99.9 (3.4), S-P-N = 118.7 (0.4), P-N-P = 133.5 (1.8), S-P-C = 107.9 (0.9), N-P-C =

Table IV. Bond Distances and Their Estimated Standard Deviations<sup>a</sup>

Atoms	Distance, Å	Atoms	Distance, Å
Mn-S(1)	2.441 (1)	C(15)-C(16)	1.347 (7)
Mn-S(2)	2.426 (1)	C(16)-C(17)	1.366 (6)
Mn-S(3)	2.457 (1)	C(17)-C(18)	1.381 (7)
Mn-S(4)	2.448 (1)	C(18)-C(13)	1.369 (6)
S(1)-P(1)	2.017 (1)	C(19)-C(20)	1.385 (4)
S(2)-P(2)	2.017 (1)	C(20)-C(21)	1.389 (4)
S(3)-P(3)	2.008 (1)	C(21)-C(22)	1.357 (6)
S(4)-P(4)	2.010 (1)	C(22)-C(23)	1.364 (5)
P(1)-N(1)	1.582 (3)	C(23)-C(24)	1.382 (5)
P(2)-N(1)	1.588 (2)	C(24)-C(19)	1.383 (5)
P(3)-N(2)	1.593 (3)	C(25)-C(26)	1.388 (4)
P(4)-N(2)	1.589 (3)	C(26)-C(27)	1.398 (6)
P(1)-C(1)	1.806 (3)	C(27)-C(28)	1.360 (6)
P(1)-C(7)	1.813 (3)	C(28)-C(29)	1.362 (5)
P(2)-C(13)	1.802 (3)	C(29)-C(30)	1.388 (5)
P(2)-C(19)	1.811 (3)	C(30)-C(25)	1.377 (5)
P(3)-C(25)	1.805 (3)	C(31)-C(32)	1.378 (5)
P(3)-C(31)	1.815 (3)	C(32)-C(33)	1.381 (5)
P(4)-C(37)	1.808 (3)	C(33)-C(34)	1.367 (6)
P(4)-C(43)	1.814 (3)	C(34)-C(35)	1.357 (6)
C(1)-C(2)	1.375 (4)	C(35)-C(36)	1.389 (5)
C(2)-C(3)	1.375 (6)	C(36)-C(31)	1.378 (4)
C(3)-C(4)	1.362 (7)	C(37)-C(38)	1.387 (4)
C(4)-C(5)	1.364 (6)	C(38)-C(39)	1.390 (6)
C(5)-C(6)	1.387 (6)	C(39)-C(40)	1.360 (7)
C(6)-C(1)	1.366 (5)	C(40)-C(41)	1.362 (5)
C(7)-C(8)	1.372 (5)	C(41)-C(42)	1.380 (5)
C(8)-C(9)	1.409 (5)	C(42)-C(37)	1.377 (5)
C(9)-C(10)	1.353 (7)	C(43)-C(44)	1.328 (5)
C(10)-C(11)	1.352 (7)	C(44)-C(45)	1.378 (6)
C(11)-C(12)	1.385 (5)	C(45)-C(46)	1.314 (7)
C(12)-C(7)	1.375 (5)	C(46)-C(47)	1.316 (7)
C(13)-C(14)	1.384 (4)	C(47)-C(48)	1.384 (5)
C(14)-C(15)	1.382 (6)	C(48)-C(43)	1.362 (5)

<sup>a</sup> The standard deviations given in parentheses refer to the last digits of the respective values. The carbon atoms attached to P(1) are C(1)<sub>eq</sub> and C(7)<sub>ax</sub>, to P(2) are C(13)<sub>eq</sub> and C(19)<sub>ax</sub>, to P(3) are C(25)<sub>eq</sub> and C(31)<sub>ax</sub>, and to P(4) are C(37)<sub>eq</sub> and C(43)<sub>ax</sub>.

107.8 (2.2), and C-P-C = 106.1 (1.3)°. The S-P, P-N, and P-C distances, as well as the nonring average bond angles about the phosphorus atoms [S-P-C, N-P-C, and C-P-C], are in agreement with corresponding values for Ni(SP(CH<sub>3</sub>)<sub>2</sub>NP(CH<sub>3</sub>)<sub>2</sub>S)<sub>2</sub><sup>2</sup> and Fe(SP(CH<sub>3</sub>)<sub>2</sub>NP(CH<sub>3</sub>)<sub>2</sub>S)<sub>2</sub><sup>3</sup>. The S-P and P-N bond lengths are consistent with a delocalized π-bond structure involving the five ligand atoms in the chelate ring, as has been noted previously.<sup>2</sup>

The packing is largely determined by intermolecular contacts among the phenyl groups. Some representative intermolecular distances are presented in Table VIII. The closest carbon-carbon contact of 3.554 Å in Mn(SPPH<sub>2</sub>NPPH<sub>2</sub>-S)<sub>2</sub> compares well with the shortest C···C distance, 3.5 Å, in Ni(SP(CH<sub>3</sub>)<sub>2</sub>NP(CH<sub>3</sub>)<sub>2</sub>S)<sub>2</sub><sup>2</sup> and Fe(SP(CH<sub>3</sub>)<sub>2</sub>NP(CH<sub>3</sub>)<sub>2</sub>S)<sub>2</sub><sup>3</sup>. Some of the shortest intermolecular distances involve carbon atoms which have unusually large amplitude of thermal vibration along one of the principal axes of the atomic vibration ellipsoid. Carbon atoms 16, 17, 44, and 45, which are bonded to hydrogen atoms 13, 14, 36, and 37, have [ $\bar{U}^2_{\text{max}}$ ]<sup>1/2</sup> values of 0.458, 0.515, 0.529, and 0.653, respectively. Some short intermolecular distances that are associated with the latter atoms are H(36)···H(37) = 2.112 Å, H(37)···H(37) = 2.413 Å, C(44)···H(14) = 2.750 Å, and C(17)···C(44) = 3.6 Å.

**Electronic Absorption Spectra of Mn(SPPH<sub>2</sub>NPPH<sub>2</sub>S)<sub>2</sub>.** The single-crystal electronic absorption spectra of Mn(SPPH<sub>2</sub>NPPH<sub>2</sub>S)<sub>2</sub> at 5.0 and 77°K are shown in Figure 2. The 77°K electronic excitation and emission spectra of a polycrystalline sample of the complex have previously

Table V. Bond Angles and Their Estimated Standard Deviations<sup>a</sup>

Atoms	Angle, deg	Atoms	Angle, deg
S(1)-Mn-S(2)	111.68 (4)	P(4)-C(43)-C(44)	121.3 (3)
S(1)-Mn-S(3)	110.82 (3)	P(4)-C(43)-C(48)	122.1 (2)
S(1)-Mn-S(4)	106.32 (4)	C(1)-C(2)-C(3)	121.4 (4)
S(2)-Mn-S(3)	107.47 (3)	C(2)-C(3)-C(4)	120.1 (3)
S(2)-Mn-S(4)	108.49 (4)	C(3)-C(4)-C(5)	119.6 (4)
S(3)-Mn-S(4)	112.08 (4)	C(4)-C(5)-C(6)	120.1 (4)
Mn-S(1)-P(1)	98.11 (4)	C(5)-C(6)-C(1)	121.0 (3)
Mn-S(2)-P(2)	104.56 (4)	C(6)-C(1)-C(2)	117.9 (3)
Mn-S(3)-P(3)	96.94 (4)	C(7)-C(8)-C(9)	119.2 (4)
Mn-S(4)-P(4)	99.80 (4)	C(8)-C(9)-C(10)	119.6 (4)
S(1)-P(1)-N(1)	118.8 (1)	C(9)-C(10)-C(11)	121.7 (4)
S(2)-P(2)-N(1)	118.6 (1)	C(10)-C(11)-C(12)	119.1 (4)
S(3)-P(3)-N(2)	118.3 (1)	C(11)-C(12)-C(7)	120.8 (4)
S(4)-P(4)-N(2)	119.2 (1)	C(12)-C(7)-C(8)	119.5 (3)
P(1)-N(1)-P(2)	134.7 (2)	C(13)-C(14)-C(15)	120.2 (4)
P(3)-N(2)-P(4)	131.9 (2)	C(14)-C(15)-C(16)	120.6 (3)
S(1)-P(1)-C(1)	107.3 (1)	C(15)-C(16)-C(17)	119.7 (4)
S(1)-P(1)-C(7)	107.6 (1)	C(16)-C(17)-C(18)	120.7 (5)
S(2)-P(2)-C(13)	107.2 (1)	C(17)-C(18)-C(13)	120.0 (3)
S(2)-P(2)-C(19)	108.9 (1)	C(18)-C(13)-C(14)	118.8 (3)
S(3)-P(3)-C(25)	109.2 (1)	C(19)-C(20)-C(21)	119.6 (3)
S(3)-P(3)-C(31)	108.6 (1)	C(20)-C(21)-C(22)	120.6 (3)
S(4)-P(4)-C(37)	107.2 (1)	C(21)-C(22)-C(23)	120.2 (3)
S(4)-P(4)-C(43)	107.3 (1)	C(22)-C(23)-C(24)	120.3 (4)
N(1)-P(1)-C(1)	105.4 (2)	C(23)-C(24)-C(19)	120.1 (3)
N(1)-P(1)-C(7)	107.6 (1)	C(24)-C(19)-C(20)	119.2 (3)
N(1)-P(2)-C(13)	107.9 (1)	C(25)-C(26)-C(27)	119.7 (4)
N(1)-P(2)-C(19)	108.3 (1)	C(26)-C(27)-C(28)	120.7 (3)
N(2)-P(3)-C(25)	105.0 (1)	C(27)-C(28)-C(29)	120.2 (4)
N(2)-P(3)-C(31)	109.9 (1)	C(28)-C(29)-C(30)	119.9 (4)
N(2)-P(4)-C(37)	105.2 (1)	C(29)-C(30)-C(25)	121.1 (3)
N(2)-P(4)-C(43)	109.7 (1)	C(30)-C(25)-C(26)	118.5 (3)
C(1)-P(1)-C(7)	106.2 (1)	C(31)-C(32)-C(33)	120.5 (3)
C(13)-P(2)-C(19)	105.0 (1)	C(32)-C(33)-C(34)	119.9 (4)
C(25)-P(3)-C(31)	105.1 (1)	C(33)-C(34)-C(35)	120.4 (3)
C(37)-P(4)-C(43)	107.6 (1)	C(34)-C(35)-C(36)	120.1 (3)
P(1)-C(1)-C(2)	121.6 (3)	C(35)-C(36)-C(31)	120.2 (3)
P(1)-C(1)-C(6)	120.5 (2)	C(36)-C(31)-C(32)	118.9 (3)
P(1)-C(7)-C(8)	120.1 (3)	C(37)-C(38)-C(39)	120.6 (4)
P(1)-C(7)-C(12)	120.4 (3)	C(38)-C(39)-C(40)	120.3 (3)
P(2)-C(13)-C(14)	120.9 (3)	C(39)-C(40)-C(41)	119.6 (4)
P(2)-C(13)-C(18)	120.2 (2)	C(40)-C(41)-C(42)	120.7 (4)
P(2)-C(19)-C(20)	122.4 (2)	C(41)-C(42)-C(37)	120.8 (3)
P(2)-C(19)-C(24)	118.5 (2)	C(42)-C(37)-C(38)	117.9 (3)
P(3)-C(25)-C(26)	121.9 (3)	C(43)-C(44)-C(45)	120.7 (4)
P(3)-C(25)-C(30)	119.5 (2)	C(44)-C(45)-C(46)	122.6 (4)
P(3)-C(31)-C(32)	121.0 (2)	C(45)-C(46)-C(47)	118.2 (4)
P(3)-C(31)-C(36)	120.1 (2)	C(46)-C(47)-C(48)	120.5 (4)
P(4)-C(37)-C(38)	121.4 (3)	C(47)-C(48)-C(43)	121.5 (3)
P(4)-C(37)-C(42)	120.7 (2)	C(48)-C(43)-C(44)	116.5 (3)

<sup>a</sup> The standard deviations given in parentheses refer to the last digits of the respective values.

Table VI. Least-Squares Planes in Bis(tetraphenyldithioimidodiphosphinato)manganese(II)<sup>a</sup>

Atom	Dev, Å	Atom	Dev, Å
(1) $-0.0237X - 0.2558Y + 0.9063Z - 1.939 = 0$			
Mn	0.0	N(1)*	0.1677
S(1)	0.0	C(1)*	0.8891
S(2)	0.0	C(7)*	2.5863
P(1)*	0.8557	C(13)*	0.0230
P(2)*	-0.4618	C(19)*	-2.2633
(2) $-0.0671X + 0.8518Y + 0.2129Z - 3.588 = 0$			
Mn	0.0	N(2)*	0.2858
S(3)	0.0	C(25)*	1.1021
S(4)	0.0	C(31)*	2.6515
P(3)*	0.9465	C(37)*	-0.2873
P(4)*	-0.5151	C(43)*	-2.2860

<sup>a</sup> Planes are defined in the real triclinic coordinates (X, Y, Z). Planes are calculated using unit weight for all atoms except those marked with an asterisk which were given zero weight.

been reported.<sup>4</sup> The excitation spectrum agrees well with the absorption spectra reported here. Although the absorp-

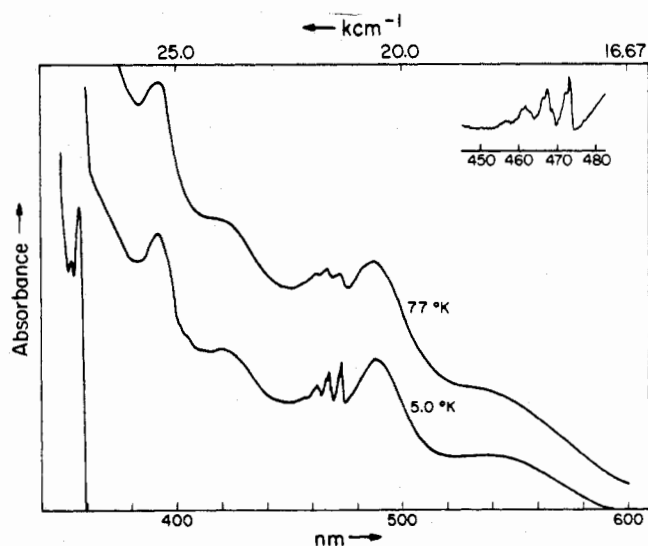


Figure 2. Single-crystal electronic absorption spectra of bis(tetraphenyldithioimidodiphosphinato)manganese(II) (crystal thickness ~0.75 mm) at 77 and 5°K.

tion maxima in a dichloromethane solution (~18,520; 20,880; 21,320; 24,100; and 25,840 cm<sup>-1</sup>) and in a pressed pellet (18,590; 20,576; 21,277; 23,810; and 25,641 cm<sup>-1</sup>) are shifted from their positions in the crystal spectra, the relative intensities of the bands do not change.

The solid-state magnetic moment ( $\mu_{\text{eff}} = 5.75 \text{ BM}$ )<sup>4</sup> establishes a high-spin d<sup>5</sup> (<sup>6</sup>A<sub>1</sub>) ground electronic state for Mn(SPPPh<sub>2</sub>NPPPh<sub>2</sub>S)<sub>2</sub>. Nine spin-forbidden sextet → quartet transitions (to <sup>4</sup>G, <sup>4</sup>D, <sup>4</sup>P, and <sup>4</sup>F states) are predicted for T<sub>d</sub> Mn(II). Assignments of the bands observed in the 5°K electronic spectrum between 14,000 and 30,000 cm<sup>-1</sup> are set out in Table IX. The assignments are based on a standard Tanabe-Sugano<sup>13</sup> calculation of transition energies.<sup>14</sup> The root-mean-square deviation between observed and calculated crystal field energies was found to be a minimum for B = 559.2, C = 3118.7, and -10Dq = 4685.6 cm<sup>-1</sup>. The -10Dq value for Mn<sup>II</sup>S<sub>4</sub> is substantially larger than that calculated (3300 cm<sup>-1</sup>)<sup>15</sup> from a detailed analysis of the electronic spectrum of MnCl<sub>4</sub><sup>2-</sup>, which is consistent with the generally higher ligand field strengths of sulfur donors.

The observed band shapes and intensities of the transitions to the excited states derived from <sup>4</sup>G are in agreement with theoretical expectation. The 18,520-cm<sup>-1</sup> band is very broad, reflecting the steep slope of E/B vs. Dq/B for <sup>6</sup>A<sub>1</sub> → <sup>4</sup>T<sub>1</sub>(<sup>4</sup>G) in the Tanabe-Sugano diagram. The <sup>6</sup>A<sub>1</sub> → <sup>4</sup>T<sub>2</sub>(<sup>4</sup>G) transition is orbitally allowed and gives rise to the most intense band in the <sup>4</sup>G group.

The electronic configuration in the <sup>4</sup>E(<sup>4</sup>G) and <sup>4</sup>A<sub>1</sub>(<sup>4</sup>G) excited states, which are accidentally degenerate in non-spin-orbit crystal field theory, is the same as the <sup>6</sup>A<sub>1</sub> ground state. The <sup>6</sup>A<sub>1</sub> → <sup>4</sup>E(<sup>4</sup>G) and <sup>6</sup>A<sub>1</sub> → <sup>4</sup>A<sub>1</sub>(<sup>4</sup>G) transitions, therefore, are independent of Dq and should give rise to sharp, structured bands. The vibrationally structured band system beginning at 21,139 cm<sup>-1</sup> fits this description well. Progressions in quanta of the totally symmetric Mn-S stretching mode (average 254 cm<sup>-1</sup>; ground state<sup>16</sup> 242 cm<sup>-1</sup>) are built on four origins at 21,139, 21,186.5, 21,272.5, and 21,346 cm<sup>-1</sup>. Inclusion of a moderate

(13) Y. Tanabe and S. Sugano, *J. Phys. Soc. Jap.*, **9**, 753, 766 (1954).

(14) Calculations were performed on an IBM 370-155 computer utilizing the strong ligand field programs written by J. Thibault.

(15) M. T. Vala, C. J. Ballhausen, R. Dingle, and S. L. Holt, *Mol. Phys.*, **23**, 217 (1972).

Table VII. Root-Mean-Square Amplitudes of Vibration (Å) along the Principal Axes of the Atomic Vibration Ellipsoids

Atom	$[\bar{U}^2_{\min}]^{1/2}$	$[\bar{U}^2_{\text{intermed}}]^{1/2}$	$[\bar{U}^2_{\max}]^{1/2}$	Atom	$[\bar{U}^2_{\min}]^{1/2}$	$[\bar{U}^2_{\text{intermed}}]^{1/2}$	$[\bar{U}^2_{\max}]^{1/2}$
Mn	0.204	0.228	0.243	C(20)	0.214	0.241	0.259
S(1)	0.209	0.223	0.255	C(21)	0.199	0.294	0.299
S(2)	0.203	0.227	0.254	C(22)	0.206	0.301	0.317
S(3)	0.190	0.228	0.282	C(23)	0.211	0.279	0.361
S(4)	0.197	0.230	0.291	C(24)	0.213	0.227	0.316
P(1)	0.185	0.208	0.220	C(25)	0.187	0.206	0.218
P(2)	0.181	0.199	0.218	C(26)	0.215	0.234	0.286
P(3)	0.193	0.195	0.214	C(27)	0.196	0.250	0.337
P(4)	0.193	0.196	0.210	C(28)	0.208	0.234	0.325
N(1)	0.185	0.215	0.254	C(29)	0.209	0.281	0.297
N(2)	0.194	0.218	0.251	C(30)	0.217	0.230	0.271
C(1)	0.187	0.202	0.230	C(31)	0.195	0.208	0.214
C(2)	0.195	0.257	0.309	C(32)	0.225	0.239	0.300
C(3)	0.189	0.289	0.337	C(33)	0.204	0.300	0.345
C(4)	0.193	0.268	0.357	C(34)	0.201	0.310	0.329
C(5)	0.208	0.278	0.399	C(35)	0.208	0.278	0.341
C(6)	0.210	0.222	0.334	C(36)	0.211	0.233	0.285
C(7)	0.200	0.222	0.258	C(37)	0.192	0.199	0.237
C(8)	0.232	0.238	0.319	C(38)	0.216	0.267	0.305
C(9)	0.236	0.275	0.374	C(39)	0.182	0.327	0.352
C(10)	0.230	0.293	0.366	C(40)	0.196	0.286	0.361
C(11)	0.224	0.341	0.389	C(41)	0.216	0.304	0.317
C(12)	0.218	0.285	0.341	C(42)	0.213	0.248	0.265
C(13)	0.186	0.198	0.253	C(43)	0.200	0.209	0.224
C(14)	0.196	0.238	0.321	C(44)	0.213	0.249	0.529
C(15)	0.188	0.266	0.372	C(45)	0.207	0.318	0.653
C(16)	0.174	0.263	0.458	C(46)	0.207	0.363	0.426
C(17)	0.179	0.275	0.515	C(47)	0.189	0.343	0.398
C(18)	0.206	0.214	0.395	C(48)	0.226	0.286	0.370
C(19)	0.189	0.206	0.218				

Table VIII. Selected Intermolecular Distances

Atoms	Distance, Å	Symmetry relation
H(36)··H(37)	2.112	-x, -y, -z
H(31)··H(40)	2.183	-x, -y, -z + 1
H(1)··H(10)	2.203	-x, -y + 1, -z + 1
H(5)··H(25)	2.349	x - 1, y, z
H(8)··H(13)	2.379	-x - 1, -y, -z + 1
H(37)··H(37)	2.413	-x, -y, -z
H(3)··H(18)	2.450	-x - 1, -y + 1, -z
C(20)··H(11)	2.610	-x - 1, -y, -z
C(28)··H(38)	2.701	-x, -y, -z
C(44)··H(14)	2.750	x - 1, y, z
C(27)··H(38)	2.755	-x, -y, -z
C(9)··C(39)	3.554	-x, -y, -z + 1
C(14)··C(20)	3.617	-x - 1, -y, -z
C(10)··C(16)	3.617	-x - 1, -y, -z + 1
C(17)··C(44)	3.632	x + 1, y, z
C(3)··C(35)	3.651	-x, -y + 1, -z + 1
C(24)··C(27)	3.701	-x, -y + 1, -z
C(3)··C(36)	3.709	-x, -y + 1, -z + 1
S(1)··C(27)	3.719	-x, -y + 1, -z
Mn··Mn	9.121	-x, -y + 1, -z

degree (>10%) of covalency into a spin-orbit crystal field calculation of tetrahedral Mn(II) gives an energy ordering  $\Gamma_6[{}^4E(^4G)] < \Gamma_8[{}^4E(^4G)] < \Gamma_7[{}^4E(^4G)] < \Gamma_8[{}^4A_1(^4G)]$ .<sup>15</sup> Thus we assign the first three origins to transitions to the three spin-orbit components of  ${}^4E(^4G)$  and the highest

(16) The Raman spectrum of a solid sample of Mn(SPP<sub>2</sub>-NPP<sub>2</sub>)<sub>2</sub> exhibits an intense band at 242 cm<sup>-1</sup>, which may be assigned to the a<sub>1</sub> Mn-S stretching fundamental. The band is not observed in the infrared spectrum of the complex. Infrared bands observed at 291 and 282 cm<sup>-1</sup> are attributable to the asymmetric Mn-S stretch,  $\nu_{t_2}$ , split by the small distortion from tetrahedral symmetry. Calculations utilizing a modified Urey-Bradley force field give  $\nu_{a_1}(\text{Mn-S}) = 247 \text{ cm}^{-1}$  and  $\nu_{t_2}(\text{Mn-S}) = 283 \text{ cm}^{-1}$  for  $K(\text{Mn-S}) = 0.95 \text{ mdyne/Å}$ ,  $H(\text{SMnS}) = 0.05 \text{ mdyne/Å}$ , and  $F(\text{S} \cdots \text{S}) = 0.05 \text{ mdyne/Å}$ . Raman spectra of powdered solids and single crystals were recorded with a Cary 81 spectrophotometer. The 632.8-nm Ne line of a 0.08-W intensity was used. Frequency shifts were calibrated with benzene and carbon tetrachloride. The infrared spectrum of a Nujol mull of the Mn(II) complex between CsI plates was measured from 500 to 200 cm<sup>-1</sup> with a Perkin-Elmer Model 225 spectrophotometer.

Table IX. Observed and Calculated Electronic Transition Energies for Mn(SPP<sub>2</sub>NPh<sub>2</sub>PS)<sub>2</sub>

${}^6A_1 \rightarrow$	Energy, cm <sup>-1</sup>		$\Delta\nu$ , cm <sup>-1</sup>	Assignment
	Obsd	Calcd <sup>a</sup>		
${}^4T_1(^4G)$	18,520	18,486		
${}^4T_2(^4G)$	20,490	20,343		
${}^4E(^4G)$	21,139	21,186		
	21,186.5		47.5	$a(\Gamma_6)$
	21,272.5		133.5	$b(\Gamma_8)$
${}^4A_1(^4G)$	21,346	21,186	207	$c(\Gamma_7)$
	21,398.5		259.5	$d(\Gamma_8)$
	21,449.5		310.5	$a + \nu(a_1)$
	21,543		404	$b + \nu(a_1)$
	21,597		458	$c + \nu(a_1)$
	21,660		521	$d + \nu(a_1)$
	21,710		571	$a + 2\nu(a_1)$
	21,786		647	$b + 2\nu(a_1)$
	21,859		720	$c + 2\nu(a_1)$
	21,881		742	$d + 2\nu(a_1)$
${}^4T_2(^4D)$	23,700	24,148		
	24,691			$a$
	24,950		259	$a + \nu(a_1)$
${}^4E(^4D)$	25,477	25,101		
${}^4T_1(^4P)$	28,011	28,058		
	28,329		318	

<sup>a</sup> Rms deviation 249 cm<sup>-1</sup>.

energy origin to  ${}^6A_1 \rightarrow {}^4A_1(^4G)$ . The 207-cm<sup>-1</sup> separation between the origins of  ${}^6A_1 \rightarrow \Gamma_6[{}^4E(^4G)]$  and  ${}^6A_1 \rightarrow \Gamma_8[{}^4A_1(^4G)]$  may be accommodated with reasonable values of spin-orbit and covalency parameters in the theoretical calculations of Vala, *et al.*<sup>15</sup> No band splitting attributable to a static tetragonal distortion is observed, which is again in agreement with theoretical predictions concerning the  ${}^4E(^4G)$  and  ${}^4A_1(^4G)$  states.

The  ${}^6A_1 \rightarrow {}^4T_2(^4D)$  transition is assigned to the broad band at 23,700 cm<sup>-1</sup>. No structure was observed<sup>15</sup> on analogous bands in MnCl<sub>4</sub><sup>2-</sup> and MnBr<sub>4</sub><sup>2-</sup>. The lack of extensive fine structure could be due to strongly overlapping vibrational progressions, originating from transitions to the spin-orbit components of the  ${}^4T_2(^4D)$  state. Evidence



of one such progression in the  $a_1$  Mn-S stretch is resolved slightly above the 23,700-cm<sup>-1</sup> peak.

The  ${}^6A_1 \rightarrow {}^4E(4D)$  band peaks at 25,477 cm<sup>-1</sup>. It is well separated from the two observed components of the  ${}^6A_1 \rightarrow {}^4T_1(4P)$  transition, which fall at 28,011 and 28,329 cm<sup>-1</sup>. No additional structure in the  ${}^6A_1 \rightarrow {}^4T_1(4P)$  system is resolved in the 5°K spectrum.

**Acknowledgments.** The authors thank Dr. R. E. Marsh for helpful discussions and Dr. S. Samson for assistance with some of the X-ray work. We also thank Dr. Charles Cowman for help in obtaining the low-temperature electronic spectra. O. S. acknowledges the National Research Council of Canada for a postdoctoral fellowship (1970-1972).

This research was supported by the National Science Foundation.

Registry No. Mn(SPP<sub>3</sub>NPP<sub>3</sub>S)<sub>2</sub>, 40362-04-7.

**Supplementary Material Available.** A listing of structure factor amplitudes will appear following these pages in the microfilm edition of this volume of the journal. Photocopies of the supplementary material from this paper only or microfiche (105 × 148 mm, 24× reduction, negatives) containing all of the supplementary material for the papers in this issue may be obtained from the Journals Department, American Chemical Society, 1155 16th St., N.W., Washington, D. C. 20036. Remit check or money order for \$7.00 for photocopy or \$2.00 for microfiche, referring to the code number INORG-74-1185.

Contribution from the Department of Chemistry,  
University of Iowa, Iowa City, Iowa 52242

## Metal Complexes as Ligands. IV.<sup>1</sup> Structures of Bis[bis(triphenylphosphine)silver(I)] Bis(1,2-dicyano-1,2-ethylenedithiolato)nickelate(II), [Ag(P(C<sub>6</sub>H<sub>5</sub>)<sub>3</sub>)<sub>2</sub>]<sub>2</sub>Ni(S<sub>2</sub>C<sub>2</sub>(CN)<sub>2</sub>)<sub>2</sub>, and of Bis[bis(triphenylphosphine)silver(I)] Bis(1,1-dicyano-2,2-ethylenedithiolato)nickelate(II), [Ag(P(C<sub>6</sub>H<sub>5</sub>)<sub>3</sub>)<sub>2</sub>]<sub>2</sub>Ni(S<sub>2</sub>C=C(CN)<sub>2</sub>)<sub>2</sub>

DIMITRI COUCOUVANIS,\*<sup>2</sup> N. C. BAENZIGER, and S. M. JOHNSON

Received October 23, 1973

AIC30778S

Bis[bis(triphenylphosphine)silver(I)] bis(1,2-dicyano-1,2-ethylenedithiolato)nickelate(II), [Ag(P(C<sub>6</sub>H<sub>5</sub>)<sub>3</sub>)<sub>2</sub>]<sub>2</sub>Ni(S<sub>2</sub>C<sub>2</sub>(CN)<sub>2</sub>)<sub>2</sub> (A), crystallizes in the monoclinic space group  $P2_1/a$  with two molecules per unit cell. The cell dimensions are  $a = 22.581$  (28) Å,  $b = 13.015$  (12) Å,  $c = 14.352$  (14) Å, and  $\beta = 119.51$  (1)°. Bis[bis(triphenylphosphine)silver(I)] bis(1,1-dicyano-2,2-ethylenedithiolato)nickelate(II), [Ag(P(C<sub>6</sub>H<sub>5</sub>)<sub>3</sub>)<sub>2</sub>]<sub>2</sub>Ni(S<sub>2</sub>C=C(CN)<sub>2</sub>)<sub>2</sub> (B), crystallizes in the monoclinic space group  $P2_1/a$  with four molecules per unit cell. The cell dimensions are  $a = 26.534$  (12) Å,  $b = 12.671$  (7) Å,  $c = 22.887$  (10) Å, and  $\beta = 105.03$  (1)°. Intensity data for both A and B were collected with a four-circle computer-controlled diffractometer using the  $\theta$ - $2\theta$  scan technique. All 48 nonhydrogen atoms in A were refined anisotropically and the 30 hydrogen atoms were included as fixed atoms. All of the 88 nonhydrogen atoms in B were refined anisotropically. Refinement by block-diagonal matrix least squares using 2124 reflections for A and 3885 reflections for B gave final  $R$  factors of 0.041 and 0.063, respectively. The geometry of the NiS<sub>4</sub> group in both structures is square. The interaction of the Ag(PPh<sub>3</sub>)<sub>2</sub><sup>+</sup> cations in both A and B occurs at the NiS<sub>4</sub> moiety and the silver atoms are located above and below the NiS<sub>4</sub> planes in a chair configuration. Average values of selected bond distances and bond angles in the (AgP<sub>2</sub>)<sub>2</sub>NiS<sub>4</sub> groups are as follows: for A, Ag-Ni, 3.010 Å; Ag-S, 2.780 Å; Ni-S, 2.181 Å; Ag-P, 2.484 Å; Ni-Ag-S, 44.0°; S-Ni-S (interligand), 88.1°; S-Ni-S (intra-ligand) 91.8°; P-Ag-P, 118.5°. For B, Ag-Ni, 2.936 Å; Ag-S, 2.797 Å (range 2.689-2.916 Å); Ni-S, 2.217 Å (range 2.212-2.224 Å); Ag-P 2.480 Å (range 2.451-2.519 Å); Ni-Ag-S, 45.4° (range 44.2-46.0°); S-Ni-S (interligand), 100.5°; S-Ni-S (intra-ligand), 79.5°; P-Ag-P, 119.5°.

### Introduction

The substitution of the inert counterions that accompany certain ionic chelates, by coordinately unsaturated charged Lewis acids, has proved to be a satisfactory approach to the synthesis of coordination oligomers.<sup>1,3</sup> The specific acid-base interactions observed in these oligomers depend primarily on (a) the availability of basic sites within the ionic chelate and (b) the intrinsic affinities of the metal ions involved for these sites. The effects of these interactions can be studied in the perturbed electronic and structural properties of either the complex acid or the complex base. An acid-base system of this type which we have studied in considerable detail deals with the M(PPh<sub>3</sub>)<sub>2</sub><sup>+</sup> (M = Ag(I), Cu(I)) adducts of a series of anionic 1,1- and 1,2-dithiolate complexes of nickel(II).<sup>4</sup> In an attempt to establish the

nature of the complex acid-complex base interactions for some of these adducts we have determined the solid-state structures of the [Ag(PPh<sub>3</sub>)<sub>2</sub>]<sub>2</sub>Ni(mnt)<sub>2</sub> and [Ag(PPh<sub>3</sub>)<sub>2</sub>]<sub>2</sub>Ni(*i*-mnt)<sub>2</sub> complexes.<sup>5</sup>

### Experimental Section

**X-Ray Diffraction Measurements. Collection and Reduction of Data.** Specific details concerning crystal characteristics and X-ray diffraction methodology are shown in Table I. For each one of the structures, a set of unit cell parameters was derived from the observed diffractometer settings  $\chi$ ,  $\phi$ , and  $2\theta$  for three independent reflections. These were refined by a least-squares technique to give the best fit between calculated and observed settings  $\chi$ ,  $\phi$ , and  $2\theta$  for 12 independent reflections carefully centered on the diffractometer. The results are shown in Table I.

Intensity data for all structures were obtained by the moving crystal-moving counter technique on an automated diffractometer. A scan speed of 1°/min  $2\theta$  was used and the background for each reflection was determined by 10-sec counts at either end of the scan range. At regular intervals (*i.e.*, 40-100 reflections) three "standard"

(1) Part III: D. Coucouvanis and D. Piltingsrud, *J. Amer. Chem. Soc.*, **95**, 5556 (1973).

(2) Alfred P. Sloan Fellow, 1972-1974.

(3) D. Coucouvanis, N. C. Baenziger, and S. H. Johnson, *J. Amer. Chem. Soc.*, **95**, 3875 (1973).

(4) M. L. Caffery and D. Coucouvanis, paper in preparation.

(5) The following abbreviations will be used throughout the text: mnt, 1,2-dicyano-1,2-ethylenedithiolate; *i*-mnt, 1,1-dicyano-2,2-ethylenedithiolate; PPh<sub>3</sub>, triphenylphosphine.